PRX QUANTUM **2**, 020322 (2021)

Optimal Quantum Thermometry with Coarse-Grained Measurements

Karen V. Hovhannisyan,[1,**,*] Mathias R. Jørgensen,[2,**,†] Gabriel T. Landi,[3,**,‡]
Álvaro M. Alhambra,[4,**,§] Jonatan B. Brask,[2,¶] and Martí Perarnau-Llobet[5,‖]

[1] *The Abdus Salam International Centre for Theoretical Physics (ICTP), Strada Costiera 11, 34151 Trieste, Italy*
[2] *Department of Physics, Technical University of Denmark, 2800 Kongens Lyngby, Denmark*
[3] *Instituto de Física da Universidade de São Paulo, São Paulo, 05314-970, Brazil*
[4] *Max-Planck-Institut für Quantenoptik, 85748 Garching, Germany*
[5] *Département de Physique Appliquée, Université de Genève, 1211 Geneva, Switzerland*

(Received 2 December 2020; revised 26 March 2021; accepted 21 April 2021; published 19 May 2021)

- ¿Con qué precisión podemos estimar la temperatura de un sistema usando mediciones de grano grueso?
- ¿Cuáles son las mediciones óptimas?
- Ejemplos con Many-Body Lattice Models

Termometría Cuántica

Topical Review

Thermometry in the quantum regime: Recent theoretical progress

Mohammad Mehboudi [1], Anna Sanpera [2,3] and Luis A. Correa [4,5,6]

Consideramos un sistema con Hamiltoniano $H = \sum_k \epsilon_k |\epsilon_k\rangle\langle\epsilon_k|$

en estado de equilibrio $\rho(T) = \sum_k \frac{e^{-\epsilon_k/k_B T}}{Z} |\epsilon_k\rangle\langle\epsilon_k|$

¿Con cuánta precisión podemos estimar la temperatura del sistema?
¿Cuál es la mejor estrategia (qué mediciones hacer)?

Mohammad Mehboudi *et al* 2019 *J. Phys. A: Math. Theor.* **52** 303001

Termometría Cuántica

Consideremos un sistema cuyo estado depende de un parámetro ξ: $\rho(\xi)$
Para ganar información sobre ξ tenemos que hacer mediciones en el sistema.

Mediciones (POVM): $\mathbf{\Pi} = \{\Pi_m\}$ $\quad p_m = \mathrm{Tr}\{\Pi_m \rho(\xi)\}$ $\quad \sum_m \Pi_m = 1$

- Mido N veces obteniendo un conjunto de resultados $\mathbf{x}$.
- Construyo un estimador $\xi_{est}(\mathbf{x})$. Estudiamos el caso donde $\langle \xi_{est}(\mathbf{x}) \rangle_{\mathbf{x}} = \xi$ (unbiased estimators)
- El error en la estimación está dado por la varianza $[\Delta \xi_{est}(\mathbf{\Pi})]^2$

Mohammad Mehboudi *et al* 2019 *J. Phys. A: Math. Theor.* **52** 303001

Termometría Cuántica

El límite a qué tan pequeño puede ser el error está dado por la regla de Cramér-Rao:

$$\Delta\xi_{est}(\mathbf{\Pi}) \geq \frac{1}{\sqrt{N\mathcal{F}(\mathbf{\Pi},\xi)}}$$

Donde $\mathcal{F}(\mathbf{\Pi},\xi)$ es la *información de Fisher* $\mathcal{F}(\mathbf{\Pi},\xi) = \langle(\partial_\xi \log p(x\,|\,\xi))^2\rangle_x = \sum_x \frac{(\partial_\xi p(x\,|\,\xi))^2}{p(x\,|\,\xi)}$

¿Cuánto varía $p(x\,|\,\xi)$ ante pequeños cambios en ξ?

Encontrar $\mathbf{\Pi}$ que maximiza $\mathcal{F}(\mathbf{\Pi},\xi)$ (minimiza el error)

Mohammad Mehboudi *et al* 2019 *J. Phys. A: Math. Theor.* **52** 303001

Termometría Cuántica

Se muestra que para estimar la temperatura la mejor estrategia es usar mediciones proyectivas en la base de la energía.

Se obtiene $\mathscr{F}(T) = \dfrac{\Delta H^2}{T^4}$ $\qquad \dfrac{\Delta T}{T} \geq \dfrac{1}{\sqrt{N C_T}}$

Mohammad Mehboudi *et al* 2019 *J. Phys. A: Math. Theor.* **52** 303001

Termometría con mediciones de grano grueso

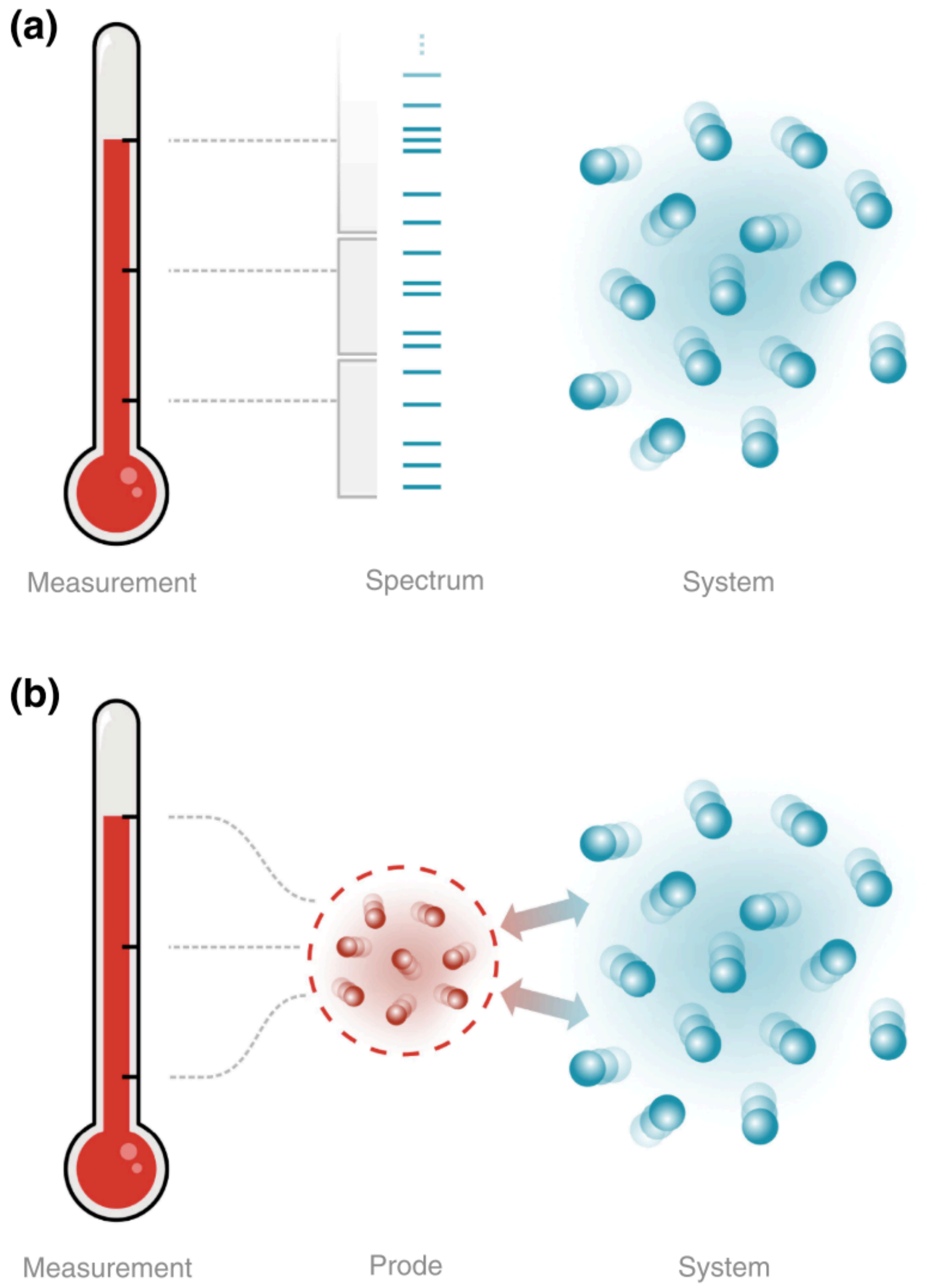

FIG. 1. (a) Thermometry with coarse-grained energy measurements. The measurement can be understood as resulting from postprocessing of a fine-grained, projective energy measurement. Energies are grouped into bins, and a single outcome is assigned to each bin. (b) Thermometry with probe-based measurements. A probe interacts unitarily with a target system. A measurement is then performed on the probe alone and used to infer the temperature of the target.

Termometría con mediciones de grano grueso

Mediciones de grano grueso: Consideran un sistema de dimensión D y mediciones con d resultados posibles. $d < D$

Consideran POVM $\mathscr{M} = \{M_\alpha\}_{\alpha=1}^{d}$ y un sistema en estado térmico $\tau = \frac{e^{-\beta H}}{Z}$

Información de Fisher de grano grueso $\mathscr{C} = \sum_{\alpha=1}^{d} \frac{1}{p_\alpha} \left(\frac{\partial p_\alpha}{\partial T} \right)^2$ con $p_\alpha = \mathrm{Tr}[M_\alpha \tau]$

$$\mathscr{C} \leq \mathscr{F}(T)$$

Encontrar $\mathscr{M}$ que maximiza $\mathscr{C}$

Medición de grano grueso óptima

Encuentran que la medición óptima consiste en agrupar los niveles de energía en bines de manera consecutiva y sin overlap.

$$M_\alpha = \sum_{E_i \in I_\alpha} |i\rangle \langle i|$$

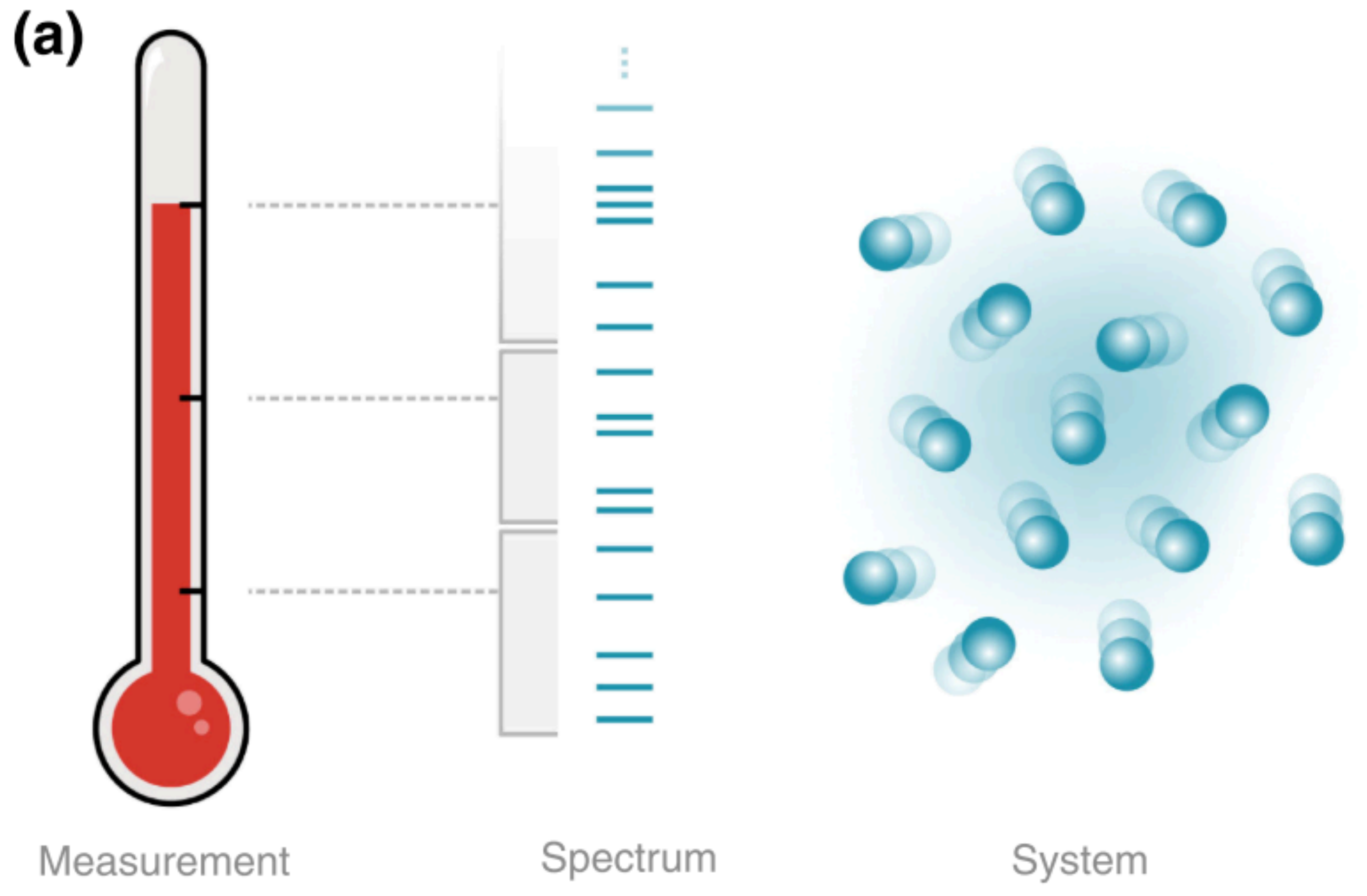

Para demostrar esto usan que sólo los elementos diagonales de M_α en la base de la energía aparecen en $\mathscr{C}$.

Bineado óptimo

$$\Omega(E) = \sum_i \delta(E - E_i) \qquad q(E) = \Omega(E)\frac{e^{-\beta E}}{Z} \longrightarrow p_\alpha = \int_{b_{\alpha-1}}^{b_\alpha} dE\, q(E) \qquad \epsilon_\alpha = \frac{1}{p_\alpha}\int_{b_{\alpha-1}}^{b_\alpha} dE\, q(E)\, E$$

La información de Fisher de grano grueso es entonces: $\mathscr{C} = \beta^4 \sum_{\alpha=1}^{d} p_\alpha (\epsilon_\alpha - \langle H \rangle)$

Definen $\mathscr{D} = \beta^4 \sum_{\alpha=1}^{d} \int_{b_{\alpha-1}}^{b_\alpha} dE\, q(E)\,(E - \epsilon_\alpha)^2$ tal que $\mathscr{F} = \mathscr{C} + \mathscr{D}$ y lo minimizan $\dfrac{\partial \mathscr{D}}{\partial b_\alpha} = 0$

$$b_\alpha = \frac{\epsilon_{\alpha+1} + \epsilon_\alpha}{2} \qquad \alpha = 1, \ldots, d-1 \qquad \text{(Ecuaciones implícitas)}$$

Ejemplos: N qubits no interactuantes

$E_g = 0$ y $E_e = 1$. Por lo tanto
$0 \leq E \leq N$ con pasos de 1.

En el caso $d = 2$ donde la medición es binaria, para N>>1 se obtiene

$$\mathscr{C} = \frac{2}{\pi} \mathscr{F}$$

Es decir, que con solamente 2 posibles resultados se recupera un 63% de la información de Fisher óptima.

Para $d = 3$ se recupera un 82%
Con el bineado óptimo

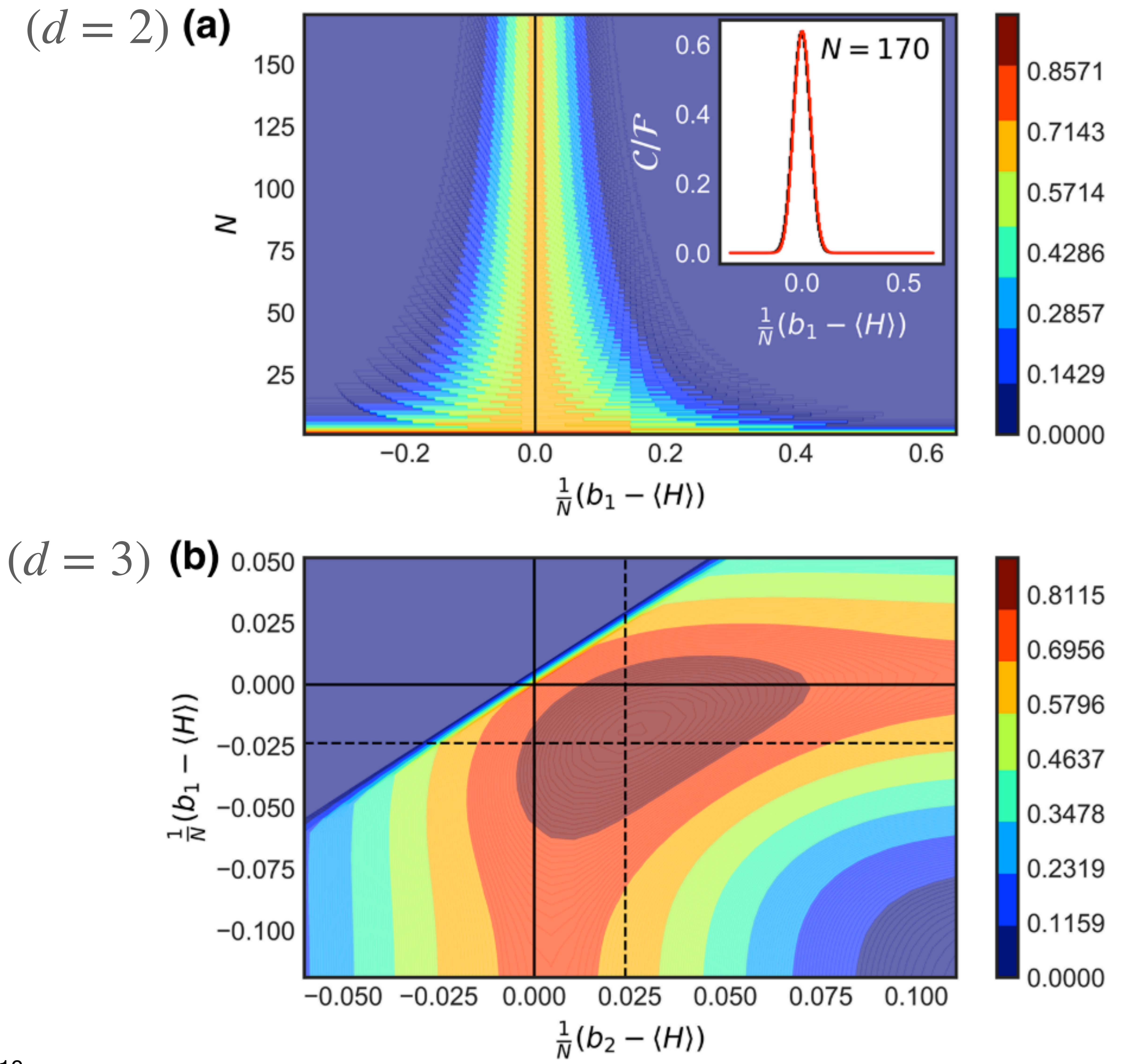

Ejemplos: Densidad de estados lineal $\Omega(E) \sim E$

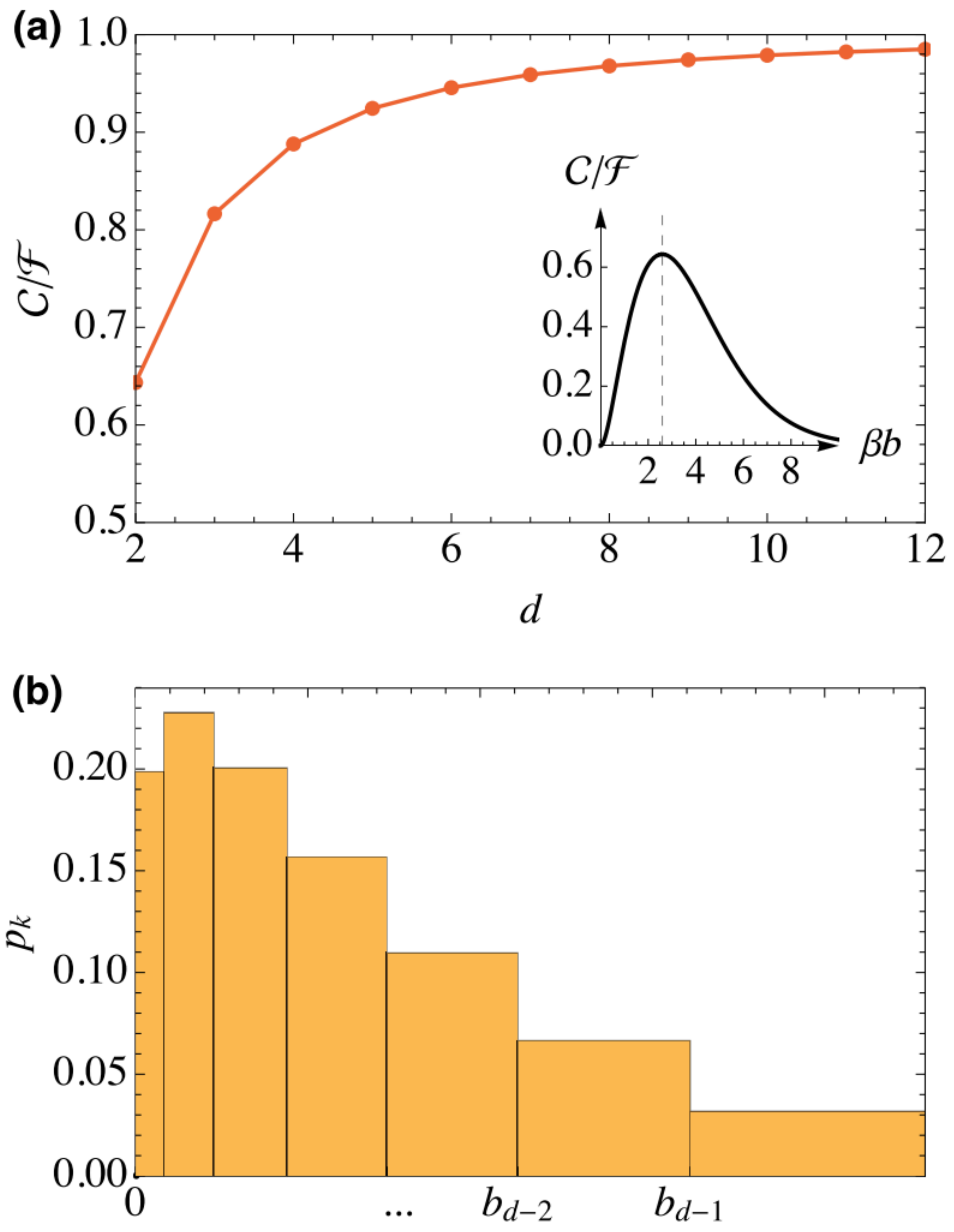

FIG. 3. Optimal thermometry binning for a system described by a linear density of states: $\Omega(E) \propto E$. (a) Optimal binned Fisher information, Eq. (17), as a function of d. The curves are normalized by the full Fisher information, which in this case reads $\mathcal{F} = 2\beta^2$. The inset shows the ratio $\mathcal{C}/\mathcal{F}$ as a function of the binning position b for $d = 2$. The optimal bin occurs at $\beta b = 2.589\,75$. The points in the main plot are already optimized over the binning positions. (b) The corresponding probabilities p_k and average bins b_k for $d = 8$.

Con 8 bins se recupera el 97% de la información de Fisher óptima.

Mediciones imperfectas

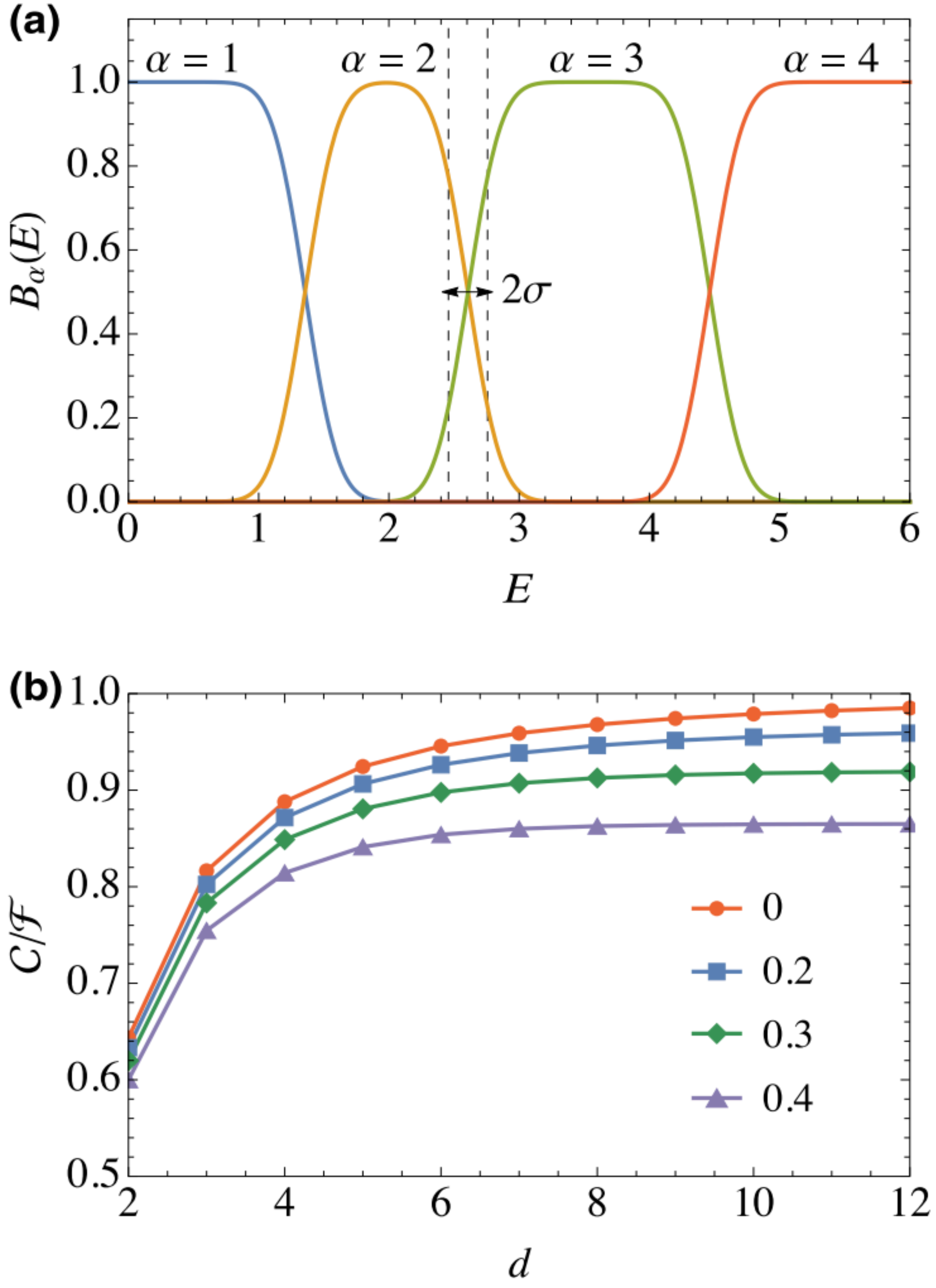

FIG. 4. The role of imperfect measurements in optimal thermometry. (a) Example of smoothed boxcars, Eq. (30), for $\sigma = 0.2$. (b) Worsening of the coarse-grained Fisher information $\mathcal{C}$ for the linear DOS example studied in Sec. III C 2. The red curve is the same as in Fig. 3(a), while the other curves are computed using the smoothed boxcars (30) with $\sigma = 0.2$, 0.3, and 0.4 (in the unit of $\beta = 1$).

$$p_\alpha = \int_{-\infty}^{\infty} dE q(E) B_\alpha(E),$$

Con un error de $\sim 30\,\%$ del ancho del bin $\dfrac{\mathscr{C}}{\mathscr{F}}$

empeora $\sim 7\,\%$

Es más robusto para bines más anchos

Many-Body Lattice Models

Cadena de Fermiones (1D)
tight-binding

$$H = \sum_{k=1}^{N} \epsilon\, c_k^\dagger c_k - \sum_{k=1}^{N} \left(c_{k+1}^\dagger c_k + c_k^\dagger c_{k+1} \right)$$

Para $d = 2$ $\quad \dfrac{\mathscr{C}}{\mathscr{F}} = \dfrac{2}{\pi} + O(\log^{-1} N)$

Este resultado es universal para modelos de Lattice que tengan distribución de energía gaussiana

1) Correlaciones decaen exponencialmente
2) Varianza en la energía escala linealmente con N

Teorema de Berry-Esseen

$N = 20$

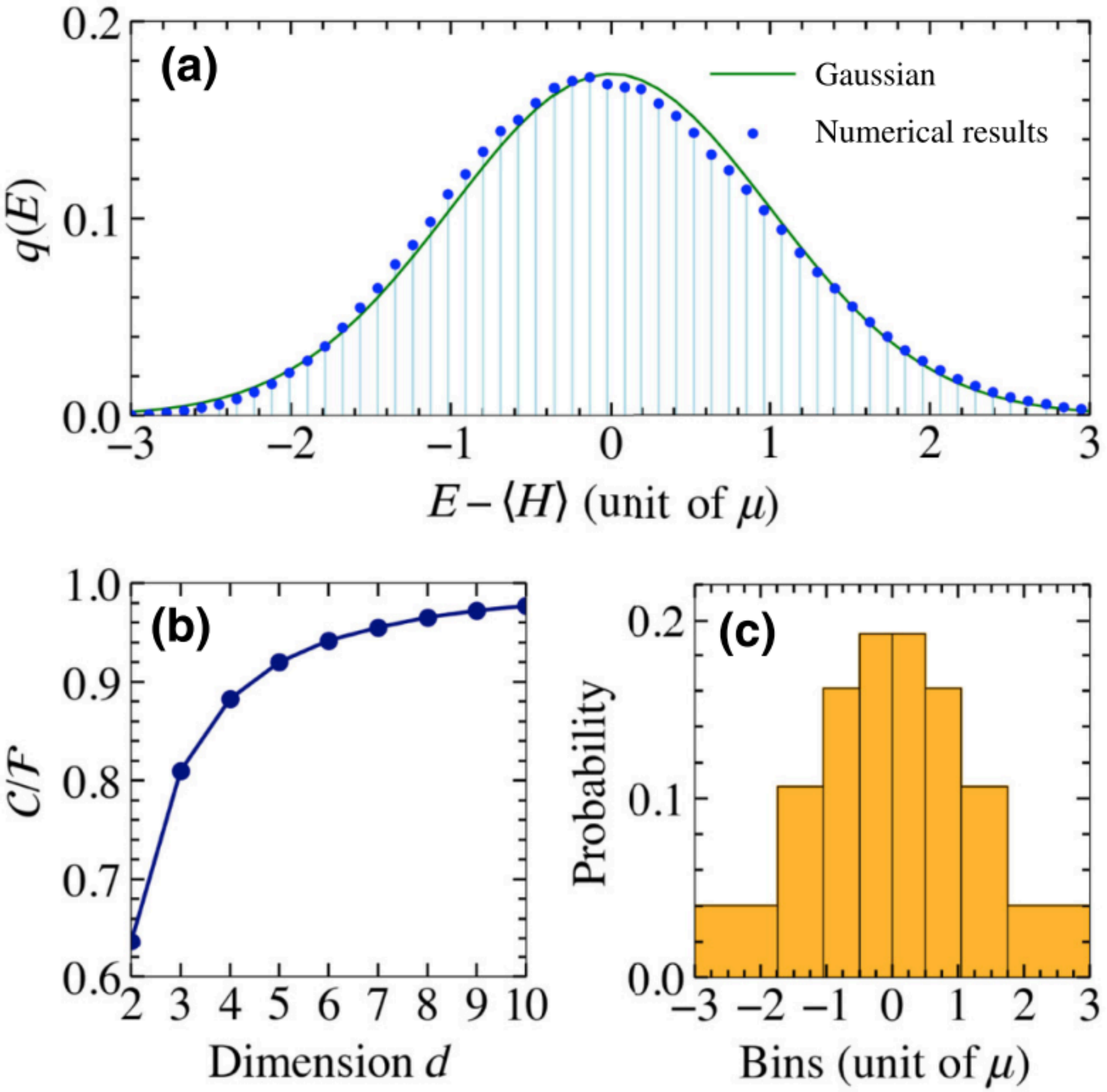

Mediciones usando una sonda

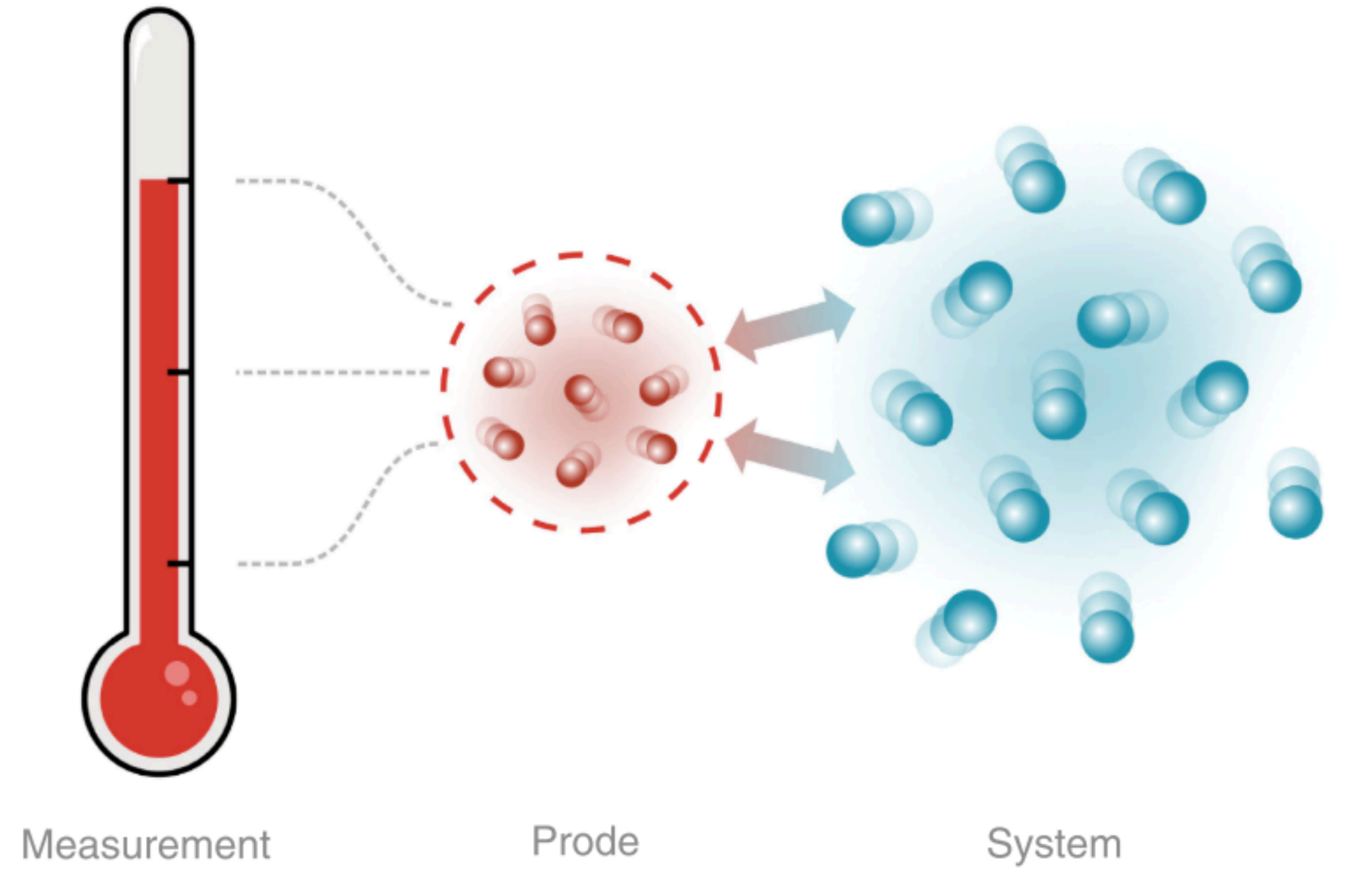

Medir usando una sonda de d dimensiones tiene la misma precisión (óptima) que usar una medición con d resultados posibles sobre el sistema

Ejemplo $d = 2$

El POVM óptimo en S se define con los bines $I_1 = \{E_j : E_j < b\}$, $I_2 = \{E_j : E_j > b\}$

Sonda:

$$H = \sum_{k=1}^{D} E_k |E_k\rangle\langle E_k| + b|\Uparrow\rangle\langle\Uparrow|$$
$$+ \lambda \sum_{E_k \leq E_D - b} (|\Downarrow\rangle\langle\Uparrow| \otimes |E_k + b\rangle\langle E_k| + \text{H.c.})$$

$$\mathbb{P}_{\Uparrow}(t) = \sin^2(\lambda t) \sum_{E_j \geq b} \frac{e^{-\beta E_j}}{Z}.$$

La probabilidad de medir al qubit en el estado excitado es equivalente a medir el bin de mayor energía en el sistema S

Undecidability in resource theory: can you tell theories apart?

Matteo Scandi[*] and Jacopo Surace[†]
ICFO-Institut de Ciencies Fotoniques, The Barcelona Institute of Science and Technology, Castelldefels (Barcelona), 08860, Spain
(Dated: May 21, 2021)

A central question in resource theory is whether one can find a set of monotones that completely characterise the allowed transitions dictated by a set of free operations. This is part of the more general problem about the possibility of certifying the equivalence of two different characterisations of the same resource theory. A similar question is whether two distinct sets of free operations generate the same class of transitions. In the present letter we prove that in the context of quantum resource theories this class of problems is undecidable in general. This is done by proving the undecidability of the reachability problem for CPTP maps, which subsumes all the other results.

PHYSICAL REVIEW E **103**, 052125 (2021)

Maximum efficiency of absorption refrigerators at arbitrary cooling power

Zhuolin Ye[1,*] and Viktor Holubec[1,2,†]
[1]*Institut für Theoretische Physik, Universität Leipzig, Postfach 100 920, D-04009 Leipzig, Germany*
[2]*Charles University, Faculty of Mathematics and Physics, Department of Macromolecular Physics, V Holešovičkách 2, CZ-180 00 Praha, Czech Republic*

(Received 25 October 2020; revised 11 March 2021; accepted 30 April 2021; published 19 May 2021)

We consider absorption refrigerators consisting of simultaneously operating Carnot-type heat engine and refrigerator. Their maximum efficiency at given power (MEGP) is given by the product of MEGPs for the internal engine and refrigerator. The only subtlety of the derivation lies in the fact that the maximum cooling power of the absorption refrigerator is not limited just by the maximum power of the internal refrigerator, but, due to the first law, also by that of the internal engine. As a specific example, we consider the simultaneous absorption refrigerators composed of low-dissipation (LD) heat engines and refrigerators, for which the expressions for MEGPs are known. The derived expression for maximum efficiency implies bounds on the MEGP of LD absorption refrigerators. It also implies that a slight decrease in power of the absorption refrigerator from its maximum value results in a large nonlinear increase in efficiency, observed in heat engines, whenever the ratio of maximum powers of the internal engine and the refrigerator does not diverge. Otherwise, the increase in efficiency is linear as observed in LD refrigerators. Thus, in all practical situations, the efficiency of LD absorption refrigerators significantly increases when their cooling power is slightly decreased from its maximum.

DOI: 10.1103/PhysRevE.103.052125

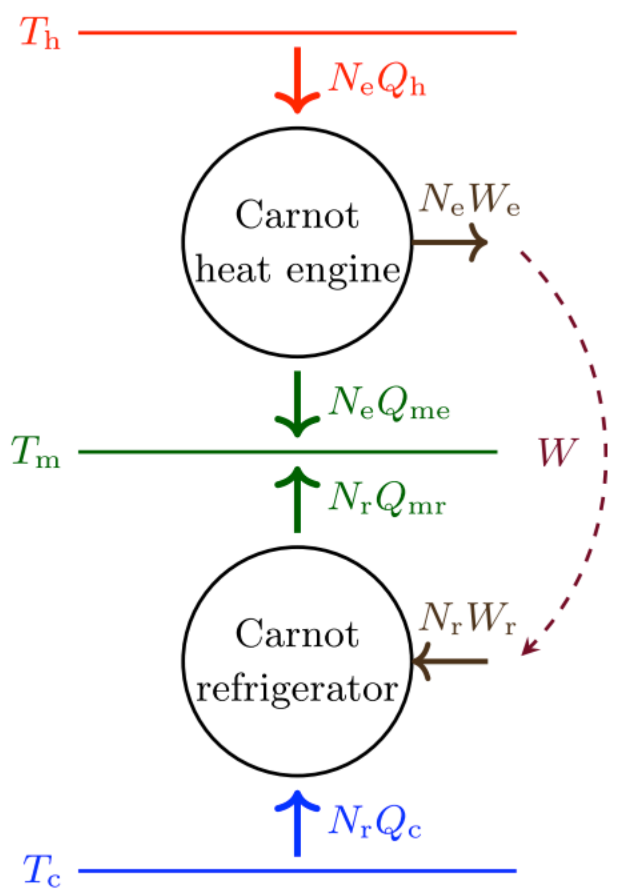

Multipartite quantum correlations in a two-mode Dicke model

Rodolfo R. Soldati,[1,2,*] Mark T. Mitchison,[3,†] and Gabriel T. Landi[1,‡]

[1]*Instituto de Física da Universidade de São Paulo, 05314-970 São Paulo, Brazil.*
[2]*Institute for Theoretical Physics I, University of Stuttgart, D-70550 Stuttgart, Germany*
[3]*School of Physics, Trinity College Dublin, College Green, Dublin 2, Ireland*

(Dated: May 21, 2021)

We analyze multipartite correlations in a generalized Dicke model involving two optical modes interacting with an ensemble of two-level atoms. In particular, we examine correlations beyond the standard bipartite entanglement and derive exact results in the thermodynamic limit. The model presents two superradiant phases involving the spontaneous breaking of either a $\mathbb{Z}_2$ or U(1) symmetry. The latter is characterized by the emergence of a Goldstone excitation, found to significantly affect the correlation profiles. Focusing on the correlations between macroscopic subsystems, we analyze both the mutual information as well as the entanglement of formation for all possible bipartitions among the optical and matter degrees of freedom. It is found that while each mode entangles with the atoms, the bipartite entanglement between the modes is zero, and they share only classical correlations and quantum discord. We also study the monogamy of multipartite entanglement and show that there exists genuine tripartite entanglement, i.e. quantum correlations that the atoms share with the two modes but that are not shared with them individually, only in the vicinity of the critical lines. Our results elucidate the intricate correlation structures underlying superradiant phase transitions in multimode systems.

PAPER

Ultimate quantum limit for amplification: a single atom in front of a mirror

Emely Wiegand[1,*], **Ping-Yi Wen**[2], **Per Delsing**[1], **Io-Chun Hoi**[3,4] and **Anton Frisk Kockum**[1,*]

1 Department of Microtechnology and Nanoscience (MC2), Chalmers University of Technology, 412 96 Gothenburg, Sweden
2 Department of Physics, National Chung Cheng University, Chiayi 621301, Taiwan
3 Department of Physics, National Tsing Hua University, Hsinchu 30013, Taiwan
4 Center for Quantum Technology, National Tsing Hua University, Hsinchu 30013, Taiwan
* Authors to whom any correspondence should be addressed.

E-mail: wiegand@chalmers.se and anton.frisk.kockum@chalmers.se

CrossMark

OPEN ACCESS

RECEIVED
23 December 2020

REVISED
19 March 2021

ACCEPTED FOR PUBLICATION
24 March 2021

PUBLISHED
20 May 2021

Keywords: quantum optics, waveguide quantum electrodynamics, circuit quantum electrodynamics, quantum mechanics, amplification

Abstract

We investigate three types of amplification processes for light fields coupling to an atom near the end of a one-dimensional (1D) semi-infinite waveguide. We consider two setups where a drive creates population inversion in the bare or dressed basis of a three-level atom and one setup where the amplification is due to higher-order processes in a driven two-level atom. In all cases, the end of the waveguide acts as a mirror for the light. We find that this enhances the amplification in two ways compared to the same setups in an open waveguide. Firstly, the mirror forces all output from the atom to travel in one direction instead of being split up into two output channels. Secondly, interference due to the mirror enables tuning of the ratio of relaxation rates for different transitions in the atom to increase population inversion. We quantify the enhancement in amplification due to these factors and show that it can be demonstrated for standard parameters in experiments with superconducting quantum circuits.

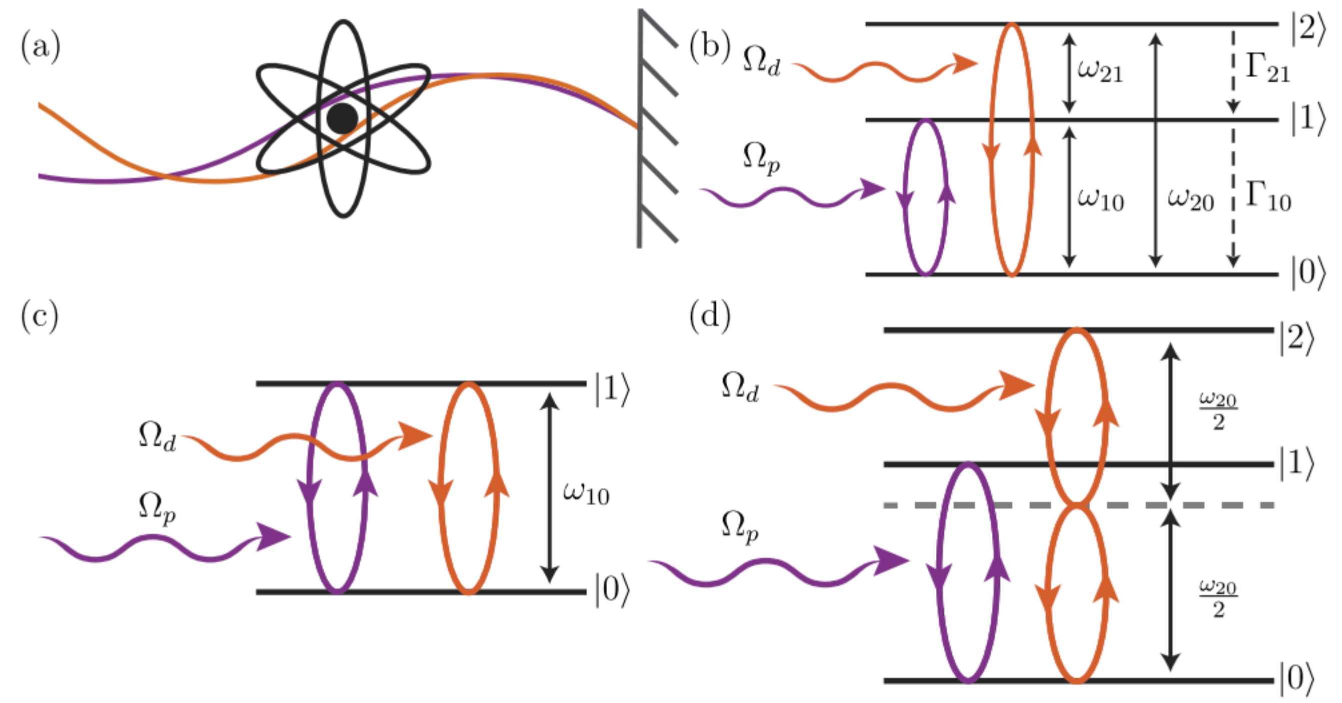

Figure 1. Sketches of the systems considered in this article. (a) All systems we study are variations on a setup with an atom in front of a mirror (short). The atom interacts with a strong drive field (orange) and a weak probe field (purple). (b) A three-level atom with transition frequencies ω_{ij} between the states $|i\rangle$ and $|j\rangle$. The atom is strongly driven with a drive amplitude Ω_d on the $|0\rangle \leftrightarrow |2\rangle$ transition. The probe field with amplitude Ω_p is applied to the $|0\rangle \leftrightarrow |1\rangle$ transition. The decay rates are denoted by Γ_{ij} for the transition from $|i\rangle$ to $|j\rangle$. (c) A two-level system both driven and probed around its transition frequency ω_{10}. (d) A three-level atom like in (b), but driven at half the frequency of the $|0\rangle \leftrightarrow |2\rangle$ transition, resulting in a two-photon driving that dresses all states of the weakly anharmonic system.

Setup	3 levels, $\omega_d = \omega_{20}$	2 levels, $\omega_d = \omega_{10}$	3 levels, $\omega_d = \omega_{20}/2$
Schematic	1(b)	1(c)	1(d)
Gain with mirror	25%	6.9%	6.2%
Gain in open waveguide	12.5%	3.4%	3%